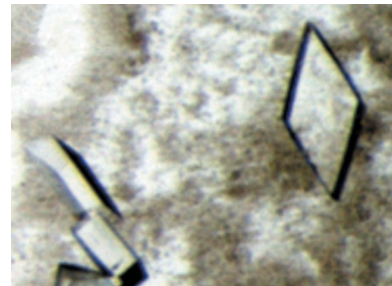


Yasutoshi Kido,<sup>a</sup> Tomoo Shiba,<sup>a</sup>  
Daniel Ken Inaoka,<sup>a</sup> Kimitoshi  
Sakamoto,<sup>a</sup> Takeshi Nara,<sup>b</sup>  
Takashi Aoki,<sup>b</sup> Teruki Honma,<sup>c</sup>  
Akiko Tanaka,<sup>c</sup> Masayuki Inoue,<sup>d</sup>  
Shigeru Matsuoka,<sup>d</sup> Anthony  
Moore,<sup>e</sup> Shigeharu Harada<sup>f\*</sup> and  
Kiyoshi Kita<sup>a\*</sup>

<sup>a</sup>Department of Biomedical Chemistry, Graduate School of Medicine, The University of Tokyo, Tokyo 113-0033, Japan, <sup>b</sup>Department of Molecular and Cellular Parasitology, Juntendo University School of Medicine, Tokyo 113-8421, Japan, <sup>c</sup>Systems and Structural Biology Center, RIKEN, Tsurumi, Yokohama 230-0045, Japan, <sup>d</sup>Graduate School of Pharmaceutical Sciences, The University of Tokyo, Tokyo 113-0033, Japan, <sup>e</sup>Biochemistry and Biomedical Sciences, School of Life Sciences, University of Sussex, Falmer, Brighton, England, and <sup>f</sup>Department of Applied Biology, Graduate School of Science and Technology, Kyoto Institute of Technology, Kyoto 606-8585, Japan

Correspondence e-mail: harada@kit.ac.jp,  
kitak@m.u-tokyo.ac.jp

Received 6 September 2009  
Accepted 15 December 2009



© 2010 International Union of Crystallography  
All rights reserved

## Crystallization and preliminary crystallographic analysis of cyanide-insensitive alternative oxidase from *Trypanosoma brucei brucei*

Cyanide-insensitive alternative oxidase (AOX) is a mitochondrial membrane protein and a non-proton-pumping ubiquinol oxidase that catalyzes the four-electron reduction of dioxygen to water. In the African trypanosomes, trypanosome alternative oxidase (TAO) functions as a cytochrome-independent terminal oxidase that is essential for survival in the mammalian host; hence, the enzyme is considered to be a promising drug target for the treatment of trypanosomiasis. In the present study, recombinant TAO (rTAO) overexpressed in haem-deficient *Escherichia coli* was purified and crystallized at 293 K by the hanging-drop vapour-diffusion method using polyethylene glycol 400 as a precipitant. X-ray diffraction data were collected at 100 K and were processed to 2.9 Å resolution with 93.1% completeness and an overall  $R_{\text{merge}}$  of 9.5%. The TAO crystals belonged to the orthorhombic space group  $I222$  or  $I2_12_12_1$ , with unit-cell parameters  $a = 63.11$ ,  $b = 136.44$ ,  $c = 223.06$  Å. Assuming the presence of two rTAO molecules in the asymmetric unit ( $2 \times 38$  kDa), the calculated Matthews coefficient ( $V_M$ ) was  $3.2 \text{ \AA}^3 \text{ Da}^{-1}$ , which corresponds to a solvent content of 61.0%. This is the first report of a crystal of the membrane-bound diiron proteins, which include AOXs.

### 1. Introduction

Cyanide-insensitive respiration in plants has been recognized since the 1920s (Moore & Siedow, 1991). Intensive biochemical studies have revealed that the mitochondrial membrane enzyme alternative oxidase (AOX) is responsible for cyanide-insensitive respiration (Moore & Siedow, 1991; Siedow & Umbach, 2000; Moore & Albury, 2008). AOX, which is cyanide-insensitive and sensitive to salicyl hydroxamic acid (SHAM), is a non-proton-pumping ubiquinol oxidase that catalyzes the four-electron reduction of dioxygen to water (Moore & Albury, 2008). AOX has been found in higher plants, algae, yeast, slime moulds, free-living amoebae, eubacteria and nematodes, as well as in protozoa, including trypanosomes (McDonald *et al.*, 2009).

*Trypanosoma brucei*, which causes African sleeping sickness in humans and nagana in livestock, which are serious health and economic problems in sub-Saharan Africa (World Health Organization, 2006), is known to show cyanide-insensitive respiration (Oppenhoes *et al.*, 1977; Chaudhuri *et al.*, 2006). In the African trypanosomes, trypanosome alternative oxidase (TAO) functions in cyanide-insensitive respiration as a cytochrome-independent terminal oxidase (Clarkson *et al.*, 1989) that is essential for survival in the mammalian host (Clayton & Michels, 1996; Chaudhuri *et al.*, 2006).

TAO is thought to be a good target for antitrypanosomal drugs because mammalian hosts do not possess this protein (Nihei *et al.*, 2002; Chaudhuri *et al.*, 2006). Indeed, we found that ascofuranone, which is isolated from the pathogenic fungus *Ascochyta visiae*, specifically inhibits the quinol oxidase activity of TAO (Minagawa *et al.*, 1997) and rapidly kills the parasites. In addition, we have confirmed the chemotherapeutic efficacy of ascofuranone *in vivo* (Yabu *et al.*, 2003, 2006).

Although TAO and other alternative oxidases (AOXs) contain diiron-binding motifs (EXXH) in their amino-acid sequences, their three-dimensional structures have not yet been elucidated (Berthold

& Stenmark, 2003; Moore & Albury, 2008). The high-resolution structure of TAO will undoubtedly have considerable implications with respect to their physicochemical mechanism, enzyme reaction and structure–function relationship, including the interaction between the enzyme and ascofuranone, which may lead to the rational design of more potent and safer antitrypanosomal drugs. Here, we describe the crystallization and preliminary crystallographic analysis of TAO.

## 2. Materials and methods

### 2.1. Preparation of rTAO

To construct the host strain FN102 for the expression of rTAO, the  $\Delta$ hemA::Km<sup>R</sup> mutation was introduced into *Escherichia coli* strain BL21 (DE3) by P1 transduction as described in a previous study (Nihei *et al.*, 2003). The strain FN102/pTbAO (Nihei *et al.*, 2003) carrying the cDNA for *T. brucei brucei* TAO was precultured at 310 K in 100 ml LB medium (containing 10 mg ampicillin, 5 mg kanamycin and 5 mg 5-aminolevulinic acid) for 4–6 h. The pre-cultured cells were grown aerobically at 303 K in 10 l S-medium [100 g tryptone peptone, 50 g yeast extract, 50 g casamino acids, 104 g K<sub>2</sub>HPO<sub>4</sub>, 30 g KH<sub>2</sub>PO<sub>4</sub>, 7.5 g trisodium citrate·2H<sub>2</sub>O, 25 g (NH<sub>4</sub>)<sub>2</sub>SO<sub>4</sub>, 0.5 g MgSO<sub>4</sub>·7H<sub>2</sub>O, 0.25 g FeSO<sub>4</sub>·7H<sub>2</sub>O, 0.25 g FeCl<sub>3</sub>, 20 g glucose and 0.1 g carbenicillin]. The culture was started at an OD<sub>600</sub> of 0.01 and expression of His<sub>6</sub>-tagged rTAO was induced by the addition of isopropyl  $\beta$ -D-1-thiogalactopyranoside (IPTG; 25  $\mu$ M) when the OD<sub>600</sub> reached 0.1. The cells were harvested 8–10 h after induction (about 40 g wet weight). The cells were then resuspended in 200 ml 50 mM Tris–HCl pH 7.5 containing 20% (w/w) sucrose, 0.1 mM phenylmethanesulfonylfluoride and protease inhibitor cocktail (Sigma) and broken using a French pressure cell at 200 MPa (Ohtake, Tokyo). Unbroken cells were removed as a pellet by centrifugation at 8000g for 10 min (Hitachi 21G). The supernatant (35 ml) was loaded onto 35 ml 50 mM Tris–HCl pH 7.5 containing 40% (w/w) sucrose and ultracentrifuged at 200 000g for 1 h at 277 K (Hitachi 85H); the fraction of inner membranes buoyant on the 40% (w/w) sucrose layer was recovered. The inner-membrane pellet was separated by further ultracentrifugation at 200 000g for 1 h (Hitachi 85H) and was re-suspended in 30 ml 50 mM Tris–HCl pH 7.5 containing 20% (w/w) sucrose. To solubilize rTAO from the membranes, the membrane suspension (35 ml) was diluted with buffer [50 mM Tris–HCl, 200 mM MgSO<sub>4</sub>, 20% (v/v) glycerol pH 7.3] at 277 K to give a 6 mg ml<sup>-1</sup> solution and 14% (w/v) *n*-octyl  $\beta$ -D-glucopyranoside (OG) was added to a final concentration of 1.4% (w/v). The solution was immediately ultracentrifuged at 200 000g for 1 h at 277 K to recover the supernatant containing the solubilized rTAO.

Cobalt-affinity chromatography was performed by a hybrid batch/column procedure using the manufacturer's instructions as stated below. 10 ml BD TALON Metal Affinity Resin (BD Bioscience) equilibrated in a batch format with 100 ml equilibration buffer [20 mM Tris–HCl, 1.4% (w/v) OG, 100 mM MgSO<sub>4</sub>, 20% (v/v) glycerol pH 7.3] was mixed with 20 ml of the OG extract for 20 min at 277 K. The resin was washed twice with 100 ml of the first wash buffer [20 mM Tris–HCl, 20 mM imidazole, 0.042% (w/v) *n*-dodecyl  $\beta$ -D-maltopyranoside (DM), 50 mM MgSO<sub>4</sub>, 20% (v/v) glycerol pH 7.3] and then transferred to a column for additional washing with 20 ml of the second wash buffer [20 mM Tris–HCl, 165 mM imidazole, 0.042% (w/v) DM, 50 mM MgSO<sub>4</sub>, 20% (v/v) glycerol pH 7.3; flow rate 1 ml min<sup>-1</sup>]. After washing, rTAO was eluted with elution buffer [20 mM Tris–HCl, 200 mM imidazole, 0.042% (w/v) DM, 50 mM MgSO<sub>4</sub>, 60 mM NaCl, 20% (v/v) glycerol pH 7.3; flow rate 1 ml min<sup>-1</sup>].

and the fractions containing rTAO as judged by activity measurements and SDS-PAGE were pooled (Kido *et al.*, 2010).

The fused N-terminal His<sub>6</sub> tag was removed from the purified rTAO using biotinylated thrombin and the tag-free rTAO was separated using streptavidin agarose (Biotinylated Thrombin Cleavage Capture Kit, Novagen) according to the manufacturer's instructions. Incubation with 10 U thrombin for 16 h at 293 K was required for the complete cleavage of 10 mg protein.

The molecular weight of the enzyme in solution was estimated by gel-filtration chromatography using a HiLoad 16/60 Superdex 200 pg column (GE Healthcare). Elution was carried out at a flow rate of 0.3 ml min<sup>-1</sup> using 50 mM Tris–HCl pH 7.4, 0.1 M NaCl, 0.042% (w/v) DM and 20% (v/v) glycerol.

### 2.2. Crystallization and X-ray data collection

The purified rTAO was concentrated to 5 mg ml<sup>-1</sup> in 20 mM Tris–HCl, 0.042% (w/v) DM, 50 mM MgSO<sub>4</sub>, 20% (v/v) glycerol pH 7.3 using an Amicon Ultra centrifugal filter device (Millipore, 30 kDa molecular-weight cutoff) and used for initial screening of crystallization conditions. Crystallization was performed by the sitting-drop vapour-diffusion technique in 96-well Corning CrystalEX microplates with a conical flat bottom (Hampton Research). In the screening, 0.5  $\mu$ l rTAO solution was mixed with an equal volume of reservoir solution and the droplet was equilibrated against 100  $\mu$ l reservoir solution at 277 and 293 K. Commercially available screening kits purchased from Hampton Research (Crystal Screen, Crystal Screen II, Crystal Screen Lite, SaltRx and MembFac), Emerald Bio-Structures (Wizard I, Wizard II, Cryo I and Cryo II) and Fluidigm (OptiMax-5 Membrane), together with homemade grid-screen reagents containing 100 mM buffer (pH 5.0–9.0), 10–40% (w/v) polyethylene glycol (PEG 400, PEG 1000, PEG 3350, PEG 6000 and PEG 10 000) and 200 mM salts (NaCl and KCl), were used as reservoir solutions. However, crystals of rTAO did not appear.

Subsequently, screening was carried out at 277 K using various detergents (DM, OG, *n*-decyld  $\beta$ -D-maltopyranoside, *n*-octyl  $\beta$ -D-maltopyranoside, *n*-nonanoyl *N*-methyl-D-glucamine, octaethylene glycol monododecylether, tetraethylene glycol monoocylether and hexaethylene glycol monododecylether). rTAO samples dissolved in different detergents were subjected to free-interface diffusion in a TOPAZ 8.96 Screening Tip against reservoir solutions purchased from TOPAZ (OptiMax-1, OptiMax-2, OptiMax-3, OptiMax-4 PEG and OptiMax-5 Membrane) using a Fluidigm TOPAZ system (Segelke, 2005). When OG was used as a detergent, several reservoir solutions containing low-molecular-weight PEGs as precipitants gave tiny crystals. The conditions were further optimized by varying the PEG (PEG 200, PEG 400 and PEG 1000) concentration (10–40%), the buffer pH (6.0–8.0), the salt type (48 salts found in PEG/Ion Screen kit from Hampton Research) and the temperature (277 and 293 K) using the sitting-drop vapour-diffusion method. However, crystals larger than 30  $\mu$ m could not be obtained and moreover they only diffracted X-rays to 7  $\text{\AA}$  resolution at most.

Next, the effects of additive detergents on crystal growth and X-ray diffraction were examined using reservoir solutions [25–40% (w/v) PEG 400, 100 mM imidazole buffer pH 6.2–7.8 and 200 mM potassium formate] supplemented with 0.1–0.5% (w/v) additive detergents. A dramatic improvement in crystal size was achieved using tetraethylene glycol monoocylether (C8E4) and the conditions, including the concentration of C8E4, were finally optimized.

Currently, crystals with average dimensions of approximately 0.1  $\times$  0.07  $\times$  0.03 mm can be reproducibly obtained at 293 K from reservoir solution consisting of 28–34% (w/v) PEG 400, 100 mM

imidazole buffer pH 7.4, 500 mM potassium formate and 0.4% (w/v) C8E4 using rTAO dissolved in 20 mM Tris-HCl pH 7.3, 0.8% (w/v) OG, 20 mM MgSO<sub>4</sub> and 20% (v/v) glycerol.

X-ray diffraction experiments were performed using synchrotron radiation on BL44XU and BL41XU at SPring-8 (Harima, Japan), BL5A and BL17A at Photon Factory and NW12A at Photon Factory Advanced Ring (Tsukuba, Japan). A crystal mounted in a nylon loop was frozen by rapidly submerging it in liquid nitrogen and X-ray diffraction patterns were recorded at 100 K. The best crystals diffracted X-rays to better than 3.0 Å resolution and a total of 180 images were recorded with an oscillation angle of 1°, an exposure time of 5 s per image and a crystal-to-detector distance of 280 mm. The data were processed and scaled using the HKL-2000 software package (Otwinowski & Minor, 1997).

### 3. Results and discussion

His<sub>6</sub>-tagged rTAO was solubilized from inner membranes using OG and was purified by cobalt-affinity chromatography in the presence of DM. After removal of the fused N-terminal His<sub>6</sub> tag, about 10 mg of enzyme was obtained from a 10 l culture. The purified rTAO, con-

**Table 1**  
Diffraction data statistics.

Values in parentheses are for the outermost resolution shell.

Space group	<i>I</i> 222 or <i>I</i> 2 <sub>1</sub> <i>2</i> <sub>1</sub>
Unit-cell parameters (Å)	<i>a</i> = 63.11, <i>b</i> = 136.44, <i>c</i> = 223.06
Beamline	SPring-8 BL41XU
Wavelength (Å)	1.000
Temperature (K)	100
Resolution (Å)	50.0–2.90 (2.95–2.90)
Total reflections	135535
Unique reflections	21720
Completeness (%)	93.1 (63.2)
<i>R</i> <sub>merge</sub> ( <i>I</i> )† (%)	9.5 (57.3)
$\langle I/\sigma(I) \rangle$	9.8 (1.7)

†  $R_{\text{merge}}(I) = \sum_{hkl} \sum_i |I_i(hkl) - \langle I(hkl) \rangle| / \sum_{hkl} \sum_i I_i(hkl)$ , where  $I_i(hkl)$  is the *i*th measurement of reflection  $hkl$ .

sisting of 329 amino-acid residues (38 kDa), was >95% pure as estimated by SDS-PAGE (Fig. 1) and its molecular weight in solution was estimated to be 110 kDa by gel-filtration chromatography. As rTAO was prepared as a water-soluble rTAO-DM complex, the complex is probably composed of a homodimer of rTAO with DM molecules bound to the hydrophobic surface of the homodimer. A homodimeric structure of TAO has also been suggested by Chaudhuri *et al.* (2005). The molecular weight of the rTAO-OG complex could not be estimated because elution of rTAO from the gel-filtration column was only successful in the presence of DM as a detergent.

After extensive screening and optimization of crystallization conditions, crystals with average dimensions of approximately 0.1 × 0.07 × 0.03 mm could be obtained within 10 d at 293 K using rTAO dissolved in 20 mM Tris-HCl pH 7.3, 0.8% (w/v) OG, 20 mM MgSO<sub>4</sub> and 20% (v/v) glycerol with a reservoir solution containing 28–34% (w/v) PEG 400, 100 mM imidazole buffer pH 7.4, 100 mM potassium formate and 0.4% (w/v) C8E4 (Fig. 2).

Analyses of the symmetry and systematic absences in the recorded diffraction patterns indicated that the crystals belonged to the orthorhombic space group *I*222 or *I*2<sub>1</sub>*2*<sub>1</sub>, with unit-cell parameters *a* = 63.11, *b* = 136.44, *c* = 223.06 Å. Assuming the presence of two rTAO molecules in the asymmetric unit (2 × 38 kDa), the calculated Matthews coefficient (*V*<sub>M</sub>) is 3.2 Å<sup>3</sup> Da<sup>-1</sup>, which corresponds to a solvent content of 61.0%. If the molecular weight of the rTAO-OG complex is presumed to be comparable to that of the rTAO-DM complex, the presence of one molecule of the rTAO-OG complex in the asymmetric unit gives a *V*<sub>M</sub> value of 2.2 Å<sup>3</sup> Da<sup>-1</sup> and a solvent content of 44.1%. A data set to 2.9 Å resolution (21 720 unique reflections) was obtained after merging 135 535 reflections recorded on 180 images, with 93.1% completeness and an overall *R*<sub>merge</sub> of 9.5%. Statistics of data collection and processing are shown in Table 1. Currently, data collection for phasing using the anomalous dispersion effect of iron is in progress. This is the first report of the crystallization of membrane-bound diiron proteins, which include AOXs.

**Figure 1**

12.5% SDS-PAGE of rTAO with Coomassie Brilliant Blue R-250 staining. Lane 1, molecular-weight markers (kDa); lane 2, rTAO purified by affinity chromatography using BD TALON Metal Affinity Resin.

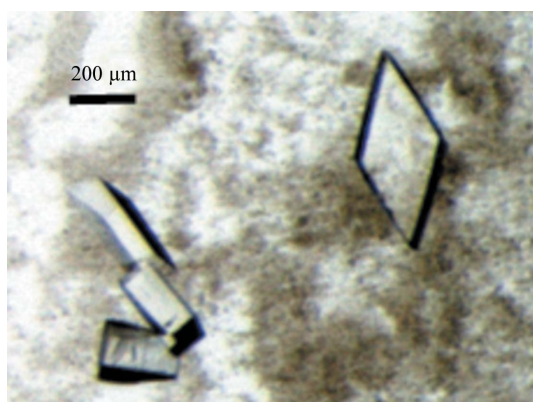


**Figure 2**

Rhombic plate-shaped crystals of rTAO obtained by the sitting-drop vapour-diffusion method using PEG 400 as a precipitant.

We thank all staff members of beamlines BL44XU and BL41XU at SPring-8, BL5A and BL17A at Photon Factory and NW12 at Photon Factory Advanced Ring for their help with X-ray diffraction data collection. This work was supported in part by grant-in-aid for Young Scientists (B) 21790402 (to YK), Creative Scientific Research Grant 18GS0314 (to KK), grant-in-aid for Scientific Research on Priority Areas 18073004 (to KK) from the Japanese Society for the Promotion of Science and the Targeted Proteins Research Program (to KK) of the Japanese Ministry of Education, Science, Culture, Sports and Technology (MEXT). ALM gratefully acknowledges the BBSRC for

financial support and, together with KK, the Prime Minister's Initiative 2 (Connect) fund for collaborative twinning.

## References

Berthold, D. A. & Stenmark, P. (2003). *Annu. Rev. Plant Biol.* **54**, 497–517.

Chaudhuri, M., Ott, R. D. & Hill, G. C. (2006). *Trends Parasitol.* **22**, 484–491.

Chaudhuri, M., Ott, R. D., Saha, L., Williams, S. & Hill, G. C. (2005). *Parasitol. Res.* **96**, 178–183.

Clarkson, A. B. Jr, Bienen, E. J., Pollakis, G. & Grady, R. W. (1989). *J. Biol. Chem.* **264**, 17770–17776.

Clayton, C. E. & Michels, P. (1996). *Parasitol. Today*, **12**, 465–471.

Kido, Y., Sakamoto, K., Nakamura, K., Harada, M., Suzuki, T., Yabu, Y., Saimoto, H., Yamakura, F., Ohmori, D., Moore, A., Harada, S. & Kita, K. (2010). *Biochim. Biophys. Acta*, doi:10.1016/j.bbabi.2009.12.021.

McDonald, A. E., Vanlerberghe, G. C. & Staples, J. F. (2009). *J. Exp. Biol.* **212**, 2627–2634.

Minagawa, N., Yabu, Y., Kita, K., Nagai, K., Ohta, N., Meguro, K., Sakajo, S. & Yoshimoto, A. (1997). *Mol. Biochem. Parasitol.* **84**, 271–280.

Moore, A. L. & Albury, M. S. (2008). *Biochem. Soc. Trans.* **36**, 1022–1026.

Moore, A. L. & Siedow, J. N. (1991). *Biochim. Biophys. Acta*, **1059**, 121–140.

Nihei, C., Fukai, Y., Kawai, K., Osanai, A., Yabu, Y., Suzuki, T., Ohta, N., Minagawa, N., Nagai, K. & Kita, K. (2003). *FEBS Lett.* **538**, 35–40.

Nihei, C., Fukai, Y. & Kita, K. (2002). *Biochim. Biophys. Acta*, **1587**, 234–239.

Oppermanns, F. R., Borst, P., Bakker, S. & Leene, W. (1977). *Eur. J. Biochem.* **76**, 29–39.

Otwinowski, Z. & Minor, W. (1997). *Methods Enzymol.* **276**, 307–326.

Segelke, B. (2005). *Expert Rev. Proteomics*, **2**, 165–172.

Siedow, J. N. & Umbach, A. L. (2000). *Biochim. Biophys. Acta*, **1459**, 432–439.

World Health Organization (2006). *Wkly Epidemiol. Rec.* **81**, 71–80.

Yabu, Y., Suzuki, T., Nihei, C., Minagawa, N., Hosokawa, T., Nagai, K., Kita, K. & Ohta, N. (2006). *Parasitol. Int.* **55**, 39–43.

Yabu, Y., Yoshida, A., Suzuki, T., Nihei, C., Kawai, K., Minagawa, N., Hosokawa, T., Nagai, K., Kita, K. & Ohta, N. (2003). *Parasitol. Int.* **52**, 155–164.